DZNep inhibits Hif-1α and Wnt signalling molecules to attenuate the proliferation and invasion of BGC-823 gastric cancer cells

RUI HUANG[1*], XIU JIN[2,3*], YONGYING GAO[4], HONGMEI YUAN[5], FEI WANG[2] and XIANGMEI CAO[2]

[1]Department of Gastroenterology, General Hospital of Ningxia Medical University; [2]Department of Pathology, Basic Medical School, Ningxia Medical University, Yinchuan, Ningxia 750004; [3]Department of Pathology, Affiliated Hospital of Jining Medical University, Jining, Shandong 272029; Departments of [4]Neurology and [5]Ultrasound, Ningxia People's Hospital, Yinchuan, Ningxia 750021, P.R. China

Received May 4, 2018; Accepted April 11, 2019

DOI: 10.3892/ol.2019.10769

Abstract. 3-deazaneplanocin A (DZNep) is a histone methyltransferase inhibitor, which may cause the reactivation of silenced tumor suppressor genes in tumors to inhibit the development, metastasis and dissemination of tumor cells. However, the effects and mechanisms of its application in gastric cancer remain unclear. The present study revealed an inhibitory function of DZNep in BGC-823 cells. The cell colony, Cell Counting Kit-8 (CCK8), wound healing, Transwell and flow cytometry assays were performed, and the results demonstrated that DZNep could inhibit the proliferation, apoptosis and invasion of BGC-823 cells, and promote their apoptosis. The effects of intervention in BDC-823 cells with DZNep on the RNA and protein expression levels of hypoxia-inducible factor (Hif-1α) and Wnt/β-catenin signalling molecules were further examined using reverse transcription-quantitative PCR and western blot analysis. The results demonstrated that different concentrations of DZNep could inhibit the expression of enhancer of zeste homolog 2 (EZH2) protein, decrease the RNA and protein expression levels of Hif-1α, total β-catenin and phosphorylated-β-catenin and increase the expression levels of non-phosphorylated-β-catenin to different degrees. The results of the present study suggests that DZNep inhibits BGC-823 gastric cancer cells via the inhibition of EZH2, Hif-1α and Wnt/β-catenin signalling molecules. These results provide theoretical basis for the application of DZNep in clinical trials.

Correspondence to: Mrs. Xiangmei Cao, Department of Pathology, Basic Medical School, Ningxia Medical University, 1160 Shenli South Street, Yinchuan, Ningxia 750004, P.R. China
E-mail: caoxm.nxmu@163.com

*Contributed equally

Key words: gastric cancer, 3-deazaneplanocin A, hypoxia inducible factor-1α, proliferation, invasion

Introduction

Gastric cancer is a common malignant tumor (1). According to the American College of Surgeons, the local or regional recurrence rate following attempted radical resection is ~40%, and the systemic recurrence rate is ~60% (2). Patients with gastric cancer develop recurrence and metastasis following surgical treatment (3).

Enhancer of zeste homolog 2 (EZH2) is an important target in the study of the inhibition of gastric cancer invasion and metastasis. Studies have reported that abnormal expression of epigenetic regulation factor polycomb group (PcG) protein is closely associated with the occurrence and development of tumors (4,5). In mammals, two main Polycomb group complexes exist-Polycomb repressive complex 1 (PRC1) and 2 (PRC2) (6). PRC2 contributes to chromatin compaction and catalyzes the methylation of histone H3 at lysine 27 (6). The core PRC2 complex, which is conserved from *Drosophila* to mammals, comprises four components: EZH1/2, SUZ12, EED and RbAp46/48 (6). EZH2 is a key member of PRC2 function that acts as a histone methyltransferase targeting lysine-27 of histone H3 (H3K27) and occurs in various malignancies, including prostate cancer, breast cancer, and glioblastoma multiforme (7). Based on its ability to modulate transcription of key genes involved in cell cycle control, DNA repair, and cell differentiation, EZH2 is believed to serve a crucial role in tissue-specific stem cell maintenance and tumor development (7). In addition, EZH2 expression can influence the expression of tumor suppressor genes, leading to malignant signalling pathways being activated, including activation of the PI3K/Akt and Wnt/β-catenin pathways (8,9).

3-deazaneplanocin A (DZNep) is an S-adenosylhomocysteine hydrolase inhibitor and a pharmacological inhibitor of histone methylation; the effect of DZNep on cancer cells is relatively specific for EZH2 (10) Studies on various malignant types of tumor have demonstrated that DZNep may serve an antitumor role via the inhibition of EZH2 (11-13); however, the underlying mechanisms remain unclear.

The microenvironment of tumor cells during growth provides stimulating signals of EZH2 expression. For example, hypoxia inducible factor 1α (Hif-1α) of the solid tumor microenvironment can induce EZH2 expression (14). During the

process of tumor evolution, Hif-1α may promote tumor cell proliferation and angiogenesis, and may cause tumor recurrence and metastasis (15). There is interactive regulation among Hif-1α and Wnt/β-catenin signalling molecules (16) and EZH2 in glioblastoma (17,18). In the present study, DZNep was used to observe the effect of DZNep on the proliferation, apoptosis, invasion and metastasis of BGC-823 gastric cancer cells, and to investigate the function of DZNep in the regulation of Hif-1α and Wnt/β-catenin signalling molecules via the inhibition of EZH2. The results of the present study provided a theoretical basis for the functions and mechanisms of inhibition of BGC-823 gastric cancer cells by DZNep.

Materials and methods

Cell culture. The poorly differentiated human gastric adenocarcinoma cell line BGC-823 was purchased from Shanghai Xin Yu Biotech Co., Ltd. BGC-823 cells were cultured in a sterile thermostatic incubator at 37˚C with 5% CO_2 in RPMI-1640 culture medium (HyClone; GE Healthcare Life Sciences) containing 10% FBS (Hangzhou Sijiqing Biological Engineering Materials Co., Ltd.) supplemented with 100 U/ml penicillin and 100 mg/ml streptomycin (HyClone; GE Healthcare Life Sciences). The culture medium was replaced every other day, and cell passage was performed every 3-4 days. Cells were cultured to the logarithmic growth phase and subsequently plated in 60 mm culture plates. BGC-823 cells were observed under an inverted microscope at x200 and x400 magnification.

Experimental groups. The cells in the experiment were divided into the DZNep group and the control group. DZNep was purchased from Sigma-Aldrich (Merck KGaA), dissolved in DMSO solution and stored at -20˚C. The DZNep stock solution (10 mM) was dissolved in phosphate-buffered saline (PBS) for cell culture. The DZNep group was incubated at 37˚C with culture medium containing 5 μM DZNep with 0.167 μl DMSO for cell colony, CCK8, wound healing, Transwell and flow cytometry assays. The control group was incubated with culture medium containing an equal volume of DMSO without DZNep.

Cell colony assay. A total of 500 cells were seeded into a 60 mm culture plate. The culture medium was replaced when the cells had stably attached. Culture medium containing DZNep or DMSO was added into the culture plate for continuous culture at 37˚C for 5, 7 or 10 days. Cells were fixed in 4% paraformaldehyde for 10 min and stained with 1% crystal violet for 20 min at room temperature. The number of visible cell colonies was counted for statistical analyses.

CCK-8 proliferation assay. CCK-8 is a kit developed by Tongren Chemical Research Institute (Dojindo Molecular Technologies, Inc.) for the detection of toxicity/proliferation of cells, which uses a water-soluble tetrazolium salt assay. The cell suspension density was adjusted to $2.5x10^4$ cells/ml using culture medium containing either DZNep or DMSO. Cells (200 μl/well) were plated into six 96-well plates. Each group had eight replicate wells. Culture medium containing 10% FBS was used as the blank control in this experiment. After 0, 6, 12, 24, 36 and 48 h, one 96-well plate was removed from the incubator, and 10 μl CCK-8 solution was added into each well. Cells were continuously cultured for another 4 h, and the absorbance (optical density) values of each well were detected using a microplate reader at 450 nm. The lowest and highest values in the experimental results were excluded, and the mean values were calculated.

Wound healing assay. A pen was used to evenly draw a line on the back of a 6-well plate, so that three lines crossed each well. Cells (~$3x10^5$) were added into each well. When the cells had stably attached and grown to ~100% confluence, a scratch perpendicular to the lines on the back of the 6-well plate was made using a pipette tip and a ruler. Cells were washed with PBS three times to remove the scratched cells. Serum-free RPMI-1640 medium containing DZNep or DMSO was added; the samples were incubated at 37˚C and images were captured at 0, 20, 25 and 44 h using a CKX41 light microscope (magnification, x100; Olympus Corporation).

Transwell invasion assay. Cell density was adjusted to $1x10^5$ cells/ml and the top chamber of the Transwell inserts was coated with Matrigel prior to the assay. Cell suspension (200 μl) was added to the top chamber, and 500 μl culture medium containing DZNep or DMSO was added to the bottom chamber of the 24-well plate. Serum-free medium was added to the upper chamber. Serum was added to the medium in the lower chamber. Cells were cultured for 24 h at 37˚C and the culture medium in the top chamber was aspirated. The cells in the top chamber were wiped off using a cotton swab. The invasive cells in the lower chamber were stained with 0.1% crystal violet for 15 min at 37˚C. An Olympus DP73 optical microscope (Olympus Corporation) was used to observe migratory cells (magnification, x200). Cells in 5-10 fields were counted, and mean values were calculated.

Reverse transcription-quantitative PCR (RT-qPCR). RT-qPCR was performed to detect and quantify the mRNA expression in the DZNep treatment groups. Total RNA in BGC-823 cells at different time points was extracted using TRIzol® (cat. no. 15596026; Thermo Fisher Scientific, Inc.), and cDNA was generated from the total RNA using a reverse transcription reagent kit (cat. no. 639505; Takara Biotechnology Co., Ltd.) for DNA amplification under the following thermocycling conditions: 3 cycles at 37˚C for 15 min, followed by 85˚C for 5 sec and hold at 4˚C. The primers used were as follows: Hif-1α forward, 5'-GAAAGC GCAAGTCTTCAAAG-3' and reverse, 5'-TGGGTAGGA GATGGAGATGC-3' (amplified fragment, 167 bp; Sangon Biotech Co., Ltd.); β-actin forward, 5'-ACACTGTGCCCA TCTACG-3' and reverse, 5'-TGTCACGCACGATTTCC-3' (amplified fragment, 152 bp). qPCR was performed using a SYBR® Green PCR kit (cat. no. KM4101; Kapa Biosystems; Roche Diagnostics). The reactions were incubated in a 96-well optical plate at 95˚C for 3 min, 95˚C for 5 sec, 56˚C for 10 sec, 72˚C for 25 sec, and 39 cycles of 65˚C for 5 sec and 95˚C for 50 sec. The $2^{-\Delta\Delta Cq}$ method was used and expression values were normalized to β-actin (19).

Western blotting. BGC-823 cells were cultured for 2, 8, 12 and 24 h with 3, 5 or 10 μM DZNep. Total protein

was extracted using a whole protein extraction reagent kit (Nanjing KeyGen Biotech Co., Ltd.). The protein concentration was determined using a bicinchoninic acid protein content detection reagent kit (Nanjing Keygen Biotech Co., Ltd.). An equal amount of protein (150 μg/lane) was separated by SDS-PAGE (8-10%). Proteins were transferred onto a nitrocellulose membrane and blocked in 10% skimmed milk at room temperature for 1-1.5 h. The membrane was incubated with the following primary antibodies: Hif-1α rabbit polyclonal antibody (cat. no. 20960-1-AP; ProteinTech Group, Inc.), EZH2 (D2C9 XP®) rabbit monoclonal antibody (mAb; cat. no. 5246; Cell Signaling Technology, Inc.), β-catenin (D10A8) XP® rabbit mAb (cat. no. 8480; Cell Signaling Technology, Inc.), non-phosphorylated (active) β-catenin (Ser45) (D2U8Y) XP® rabbit mAb (N-P-β-catenin; cat. no. 19807; Cell Signaling Technology, Inc.), β-actin (8H10D10) mouse mAb (cat. no. 3700; Cell Signaling Technology, Inc.) and phosphorylated-β-catenin (P-β-catenin; cat. no. sc-16743-R; Santa Cruz Biotechnology, Inc.); diluted at 1:1,000 in antibody dilution buffer at 4˚C overnight. The membrane was incubated with goat anti-mouse immunoglobulin G (IgG; 1:5,000; cat. no. TA130005; OriGene Technologies, Inc.) or goat anti-rabbit IgG (1:5,000; cat. no. TA130024; OriGene Technologies, Inc.) secondary antibody at room temperature for 0.5-1 h. The bands were developed using the ECL chemiluminescence reagent (ECL kit; cat. no. KGP1121; Nanjing KeyGen Biotech Co., Ltd.) for 1 min and visualized with an Amersham Imager 600 instrument (GE Healthcare Life Sciences). Densitometric analysis was performed using Image-Pro Plus version 6.0 (Media Cybernetics, Inc.).

Flow cytometry. A total of $6x10^5$ cells were added into each well of a 6-well plate. Following stable attachment of the cells, the culture medium was replaced with culture medium containing either DZNep or DMSO for 24 h. Subsequently, cells were digested, centrifuged in 800 x g at 4˚C for 5 min and transferred to a new centrifuge tube. A total of 400 μl 1X binding buffer was added to each tube and mixed evenly. A total of 5 μl Annexin V-FITC was added, gently mixed and incubated at 4˚C in the dark for 15 min. Finally, 10 μl propidium iodide was added, gently mixed and incubated at 4˚C in the dark for 5 min. Cells were detected within 30 min using a FACScalibur flow cytometer and CellQuest software (BD Biosciences).

Statistical analysis. Experiments were performed in triplicate. The results are presented as the mean ± standard deviation. Differences between two groups were compared using an unpaired Student's t-test. For multiple groups, statistical significance was analysed using one-way analysis of variance followed by a Bonferroni comparison post hoc test. Analysis was performed using SPSS version 17.0 software (SPSS, Inc.). $P<0.05$ was considered to indicate a statistically significant difference.

Results

DZNep reduces proliferation and colony formation in gastric cancer cells. Following treatment with 5 μM DZNep, BGC-823 cells were observed under an inverted microscope. The results demonstrated that cells exhibited morphological changes after 24 h. In the control group, cells were plump, had round and smooth edges, and had an orderly arrangement. In the DZNep group, cells became thin, long and thread-shaped with a small circular terminal, and cells were arranged loosely (Fig. 1A). CCK-8 proliferation experiment results demonstrated that after 6, 12, 36, and 48 h of DZNep-treatment, the proliferation activity of BGC-823 cells was significantly lower compared with that in the control group (Fig. 1B). Cell colony formation results illustrated that the number of cell colonies in the DZNep group was significantly lower compared with that in the control group, and the differences on days 5 and 7 were statistically significant (Fig. 1C). Overall, these results suggest that DZNep inhibits the proliferation and colony formation abilities of BGC-823 cells.

Wound healing is reduced by DZNep treatment. Scratch treatment in the DZNep (5 μM) and control groups was performed at the same time. The width of the cell scratch at the same location was measured after 0, 20, 25 and 44 h. Over time, cells gradually spread from the scratch edge and grew to the edge of the other side, thus gradually reducing the distance between the residual scratches. The results demonstrated that the distance between residual scratches in the DZNep intervention group was significantly wider compared with that in the control group (Fig. 2), which suggests that DZNep reduced the migration ability of the cells.

DZNep reduces the invasion ability of gastric cancer cells. Following 2, 6, 12 and 24 h of DZNep treatment (5 μM) of BGC-823 cells, numbers of cells that passed through the Transwell membranes were observed. The results demonstrated that there was no obvious movement of cells through the membrane after 2 h in the control and DZNep groups. At 6 h, a small number of cells in the DZNep and control groups passed through the membrane. At 12 and 24 h, the number of cells that passed through the membrane in the control group was significantly higher compared with that in the DZNep group (Fig. 3). The results suggest that DZNep reduced the invasive ability of the cells.

DZNep promotes BGC-823 cell apoptosis. Following 24 h of 5 μM DZNep treatment of BGC-823 cells, flow cytometry analysis revealed that the apoptotic rate was 2.5% in the DZNep group and 0.7% in the control group (Fig. 4), suggesting that DZNep promoted apoptosis.

DZNep inhibits mRNA and protein expression of Hif-1α. Detection of Hif-1α mRNA expression in BGC-823 cells after 4, 8 and 24 h following 1 and 5 μM DZNep treatment was performed by RT-qPCR. The internal control used was β-actin. The results demonstrated that following 4 h of treatment with 1 and 5 μM DZNep, and after 24 h with 5 μM DZNep, Hif-1α was significantly decreased by DZNep treatment. At 8 h, 1 μM DZNep slightly increased Hif-1α expression compared with the control group, but the change was non-significant; this suggested that the increase in Hif-1α reactivity may be transient (Fig. 5A).

Detection of Hif-1α protein expression was performed by western blot analysis. The internal control was β-actin.

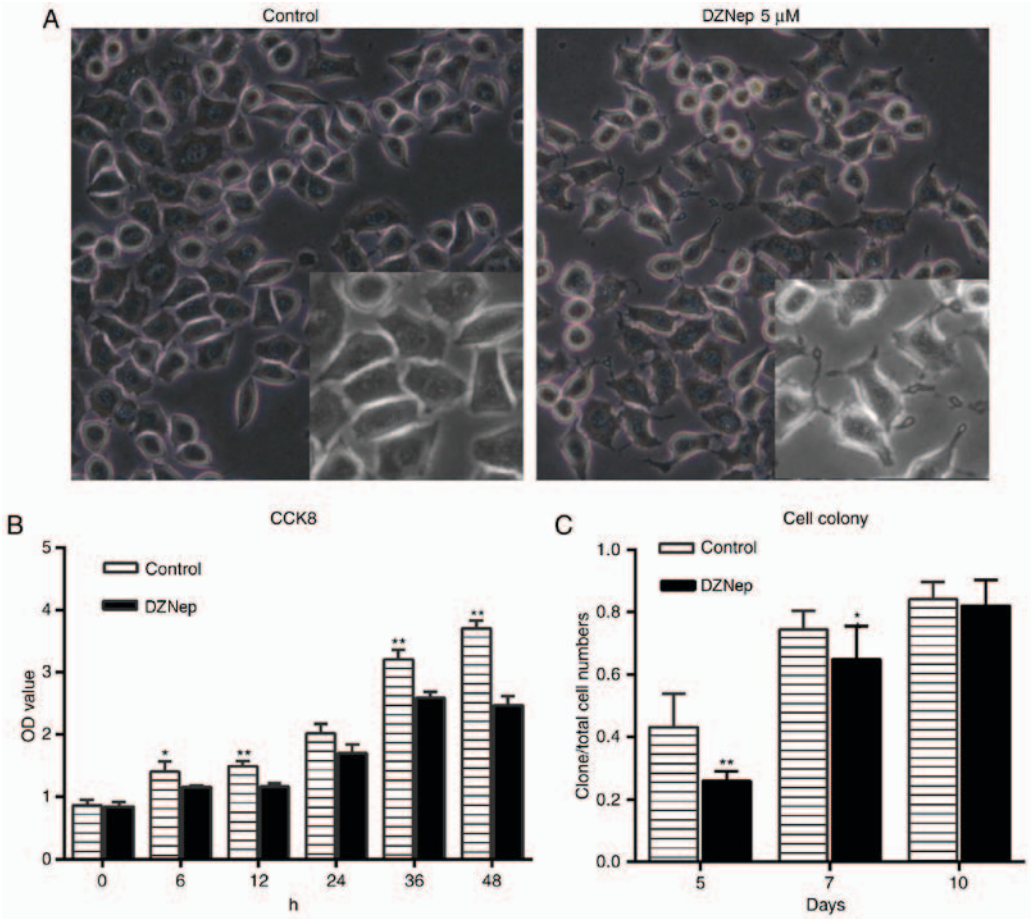

Figure 1. DZNep reduces proliferation and colony formation of BGC-823 cells. (A) Compared with cells in the control group, cells in the DZNep group became thin and long, and exhibited a thread-like shape with a small circular terminal, and the arrangement of the cells became loose (magnification, x200 and x400). (B) In the CCK-8 assay, the absorbance of the DZNep group was significantly lower compared with that of the control group at 6 and 48 h. *P<0.05, **P<0.01 vs. respective DZNep group. (C) The number of colonies in the DZNep group was significantly lower compared with that in the control group at 5 and 7 days. *P<0.05, **P<0.01 vs. respective control group. CCK-8, Cell Counting kit-8; DZNep, 3-deazaneplanocin A; OD, optical density.

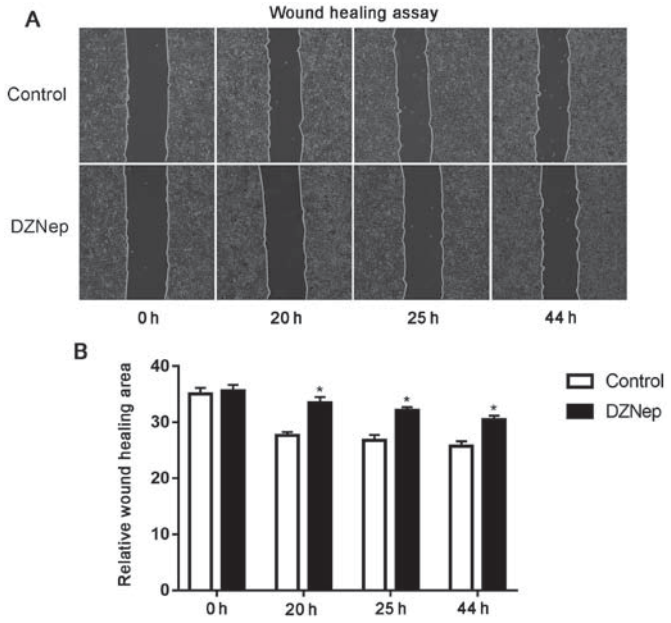

Figure 2. Wound healing is reduced following DZNep-treatment. (A) After 0, 20, 25 and 44 h, the distance between residual scratches in the DZNep group was wider compared with that in the control group (magnification, x100). (B) Bar graph summarizing numerical results with standard deviations. *P<0.05 vs. respective DZNep group. DZNep, 3-deazaneplanocin A.

Following treatment with 3, 5 and 10 μM DZNep for 24 h, western blotting demonstrated that 3, 5 and 10 μM DZNep significantly reduced the protein expression level of Hif-1α. The alterations in the protein expression levels of Hif-1α after 2, 12 and 24 h of 5 μM DZNep treatment indicated that the Hif-1α protein expression levels at each time point were significantly reduced (Fig. 5B-D).

Inhibitory function of DZNep on EZH2 and β-catenin proteins. The inhibitory function of 3, 5 and 10 μM DZNep treatment for 2, 8, 12 and 24 h on the protein expression levels of EZH2, P-β-catenin and N-P-β-catenin in BGC-823 cells was detected using western blot analysis. Compared with the control group, EZH2 protein expression significantly decreased at 8, 12 and 24 h in the 5 μM DZNep group, and P-β-catenin significantly decreased at 2, 8, 12 and 24 h in the 5 μM DZNep group. In addition, N-P-β-catenin expression significantly increased after 2, 8 and 24 h in the 5 μM DZNep group compared with the control group. Treatment with 3, 5 and 10 μM DZNep for 24 h significantly decreased the EZH2 protein expression level. In addition, 5 and 10 μM DZNep treatment decreased the total β-catenin protein level (Fig. 6). These results suggested that DZNep inhibited EZH2 protein expression and further inhibited the phosphorylation of β-catenin.

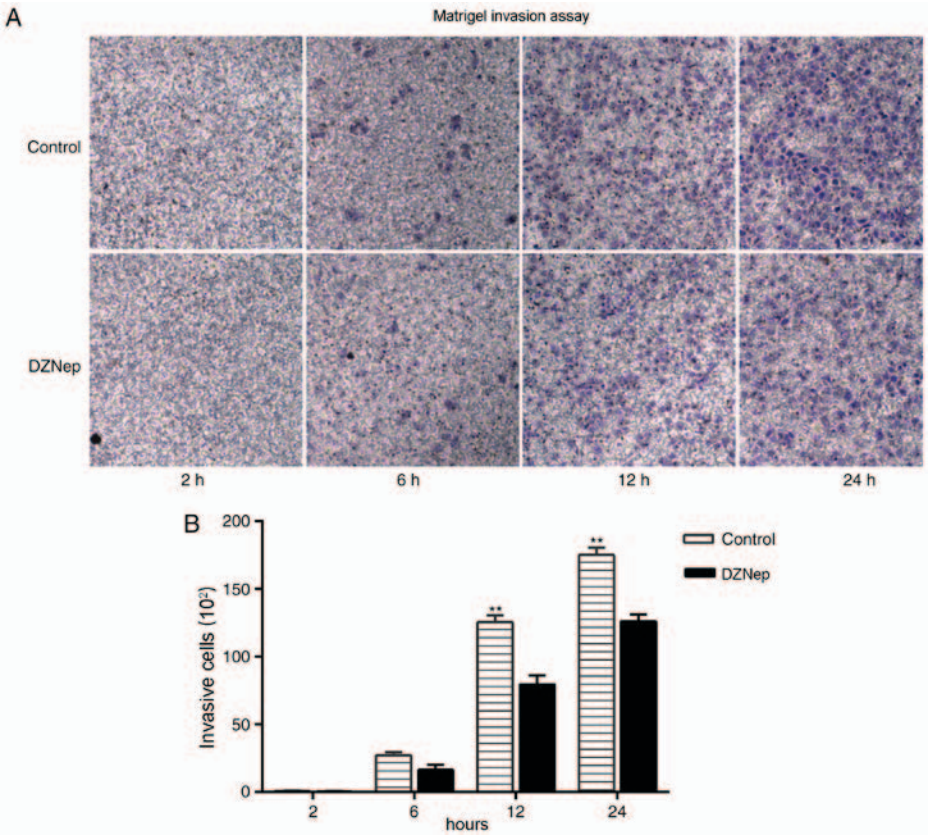

Figure 3. DZNep reduces the invasive ability of BGC-823 cells. (A) After 2, 6, 12 and 24 h, the numbers of cells that passed through the membrane in the DZNep group were markedly lower compared with that in the control group (magnification, x200). (B) Bar graph summarizing the numerical results with standard deviations. The differences after 12 and 24 h in the DZNep group were statistically significant. **P<0.01 vs. respective DZNep group. DZNep, 3-deazaneplanocin A.

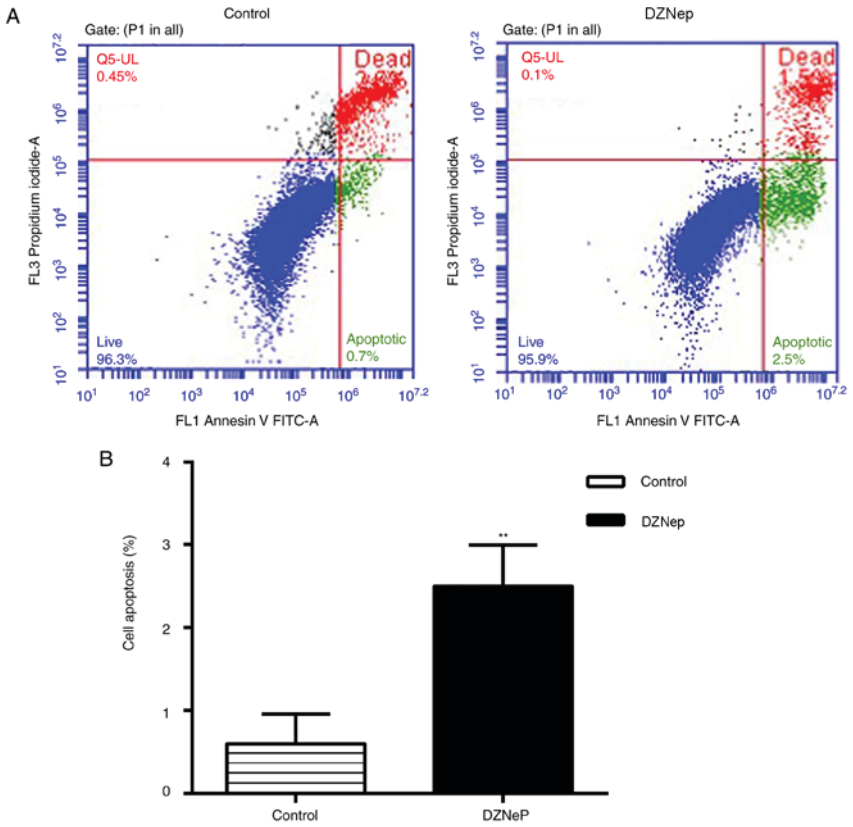

Figure 4. Apoptosis was determined by flow cytometry. (A) Apoptotic rates in the DZNep group were 2.5%, which was higher compared with those in the control group (0.7%). (B) Bar graph (mean + standard deviation) of the flow cytometry results. **P<0.01 vs. control. DZNep, 3-deazaneplanocin A.

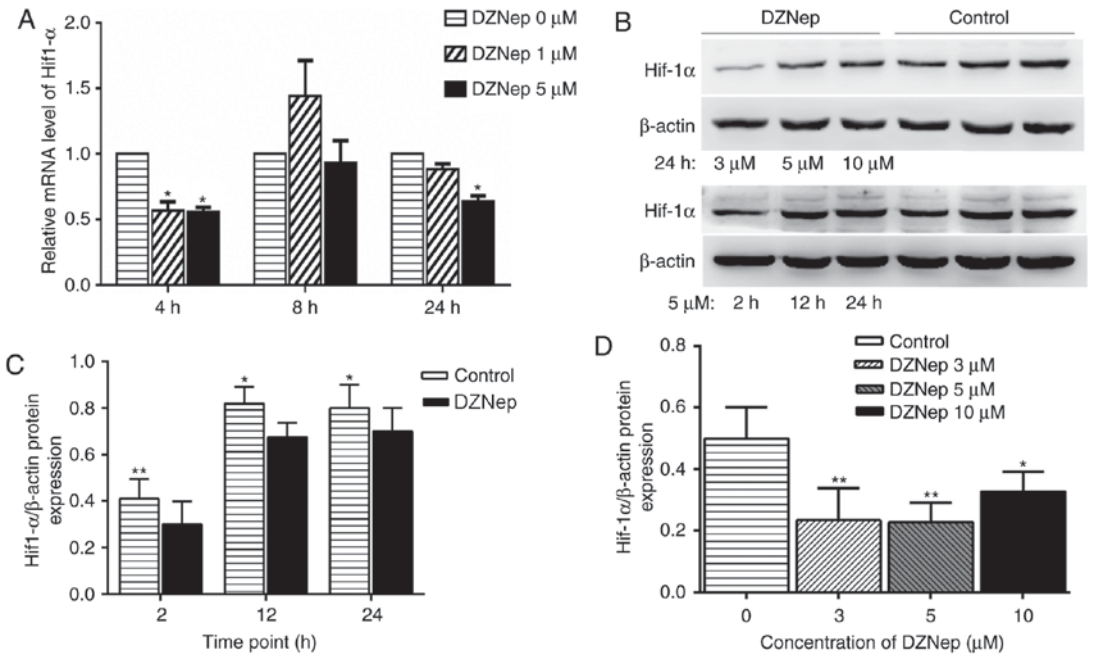

Figure 5. DZNep-treatment reduces Hif-1α gene and protein expression. (A) Hif-1α relative mRNA expression levels in BGC-823 cells after 4, 8 and 24 h treatment with 1 and 5 μM DZNep were detected by reverse transcription-quantitative PCR. Following 4 h of treatment with 1 and 5 μM DZNep, and 24 h with 5 μM DZNep, Hif-1α expression was significantly reduced. *P<0.05 vs. respective DZNep 0 μM group. (B) Effects of 3, 5 and 10 μM DZNep treatment on Hif-1α protein expression levels after 24 h were detected using western blotting. The control group was treated with DMSO. The internal control was β-actin. (C) Hif-1α protein expression levels after 2, 12 and 24 h treatment with 5 μM DZNep decreased at each time point, and the differences were statistically significant. *P<0.05, **P<0.01 vs. control. (D) DZNep treatment (3, 5 and 10 μM) significantly decreased the protein expression levels of Hif-1α, and the differences were statistically significant. *P<0.05 and **P<0.01 vs. control. DZNep, 3-deazaneplanocin A; Hif-1α, hypoxia-inducible factor 1α.

Discussion

The abnormal expression of the epigenetic regulatory factors PcG proteins is closely associated with the development and progression of tumors. Based on their different functions, PcG proteins are divided into two protein complexes, PRC1 and PRC2. PRC2 is a highly conserved histone methyltransferase that functions on the K27 lysine site of histone H3 (H3K27me3). The core component, EZH2, has histone methyltransferase activity and may catalyse the methylation of the H3K27me3 histone to inhibit target gene expression, thus resulting in tumor development (4,20,21). In gastric cancer cells, EZH2 is involved in the regulation of cell cycle-associated proteins to promote the proliferation and metastasis of gastric cancer cells (22). A previous study reported that clinical trials evaluating EZH2-targeting agents, including DZNep, should consider stratifying patients with gastric cancer by their TP53 genomic status (23). EZH2 is an important target in the study of gastric cancer invasion and metastasis. DZNep may reduce EZH2 protein expression levels, reduce H3K27me3 levels, activate PRC2 target genes and may specifically induce tumor cell apoptosis (24).

Abnormal proliferation is a common feature of malignant tumors. DZNep has been confirmed to be able to inhibit the proliferation of Eca109 oesophageal squamous cell carcinoma cells and HTC116 colorectal cancer cells (25,26). The present study used the poorly differentiated human BGC-823 gastric adenocarcinoma cell line. The CCK-8 experiment results demonstrated that DZNep inhibited BGC-823 cell proliferation. The colony formation assay results demonstrated that DZNep reduced the number of colonies formed in BGC-823 cells. The flow cytometry results demonstrated that DZNep promoted BGC-823 cell apoptosis. Notably, BGC-823 cells exhibited morphological alterations following DZNep treatment. The cell edges became sharp, and the margins exhibited thread-like and circular structures. These morphological alterations may allow cells to better attach onto the culture plate. Therefore, it was speculated that DZNep may attenuate the invasion and metastasis abilities of cells. Subsequently, wound-healing experiments and Transwell invasion experiments were performed to investigate this. The results of these assays demonstrated that DZNep attenuated the wound healing activity of BGC-823 cells and reduced the number of cells that passed through the membrane, suggesting that DZNep inhibited the invasion and metastasis of human BGC-823 gastric cancer cells.

To further study the mechanisms, it was considered that during the process of tumor progression, the blood vessel network cannot be rapidly established due to the rapid proliferation of tumor cells, thus causing a reduction in the oxygen content in the microenvironment, a lack of nutritional substances and an accumulation of acidic substances (27,28). In a hypoxic microenvironment, tumor cells are prone to develop invasion and metastasis abilities and activate drug-resistance genes to increase their adaptive ability (29,30). Hif-1 is a nuclear protein with transcriptional activity. Under the hypoxic growth environment of tumors, Hif-1 can promote tumor cell proliferation and angiogenesis to cause tumor recurrence and metastasis at the late stages and attenuate the sensitivity of tumors to chemotherapy and radiotherapy (31). Hif-1 is a heterodimeric transcription factor activated by hypoxia composed of two different subunits, HIF-1α and ARNT (aryl receptor nuclear

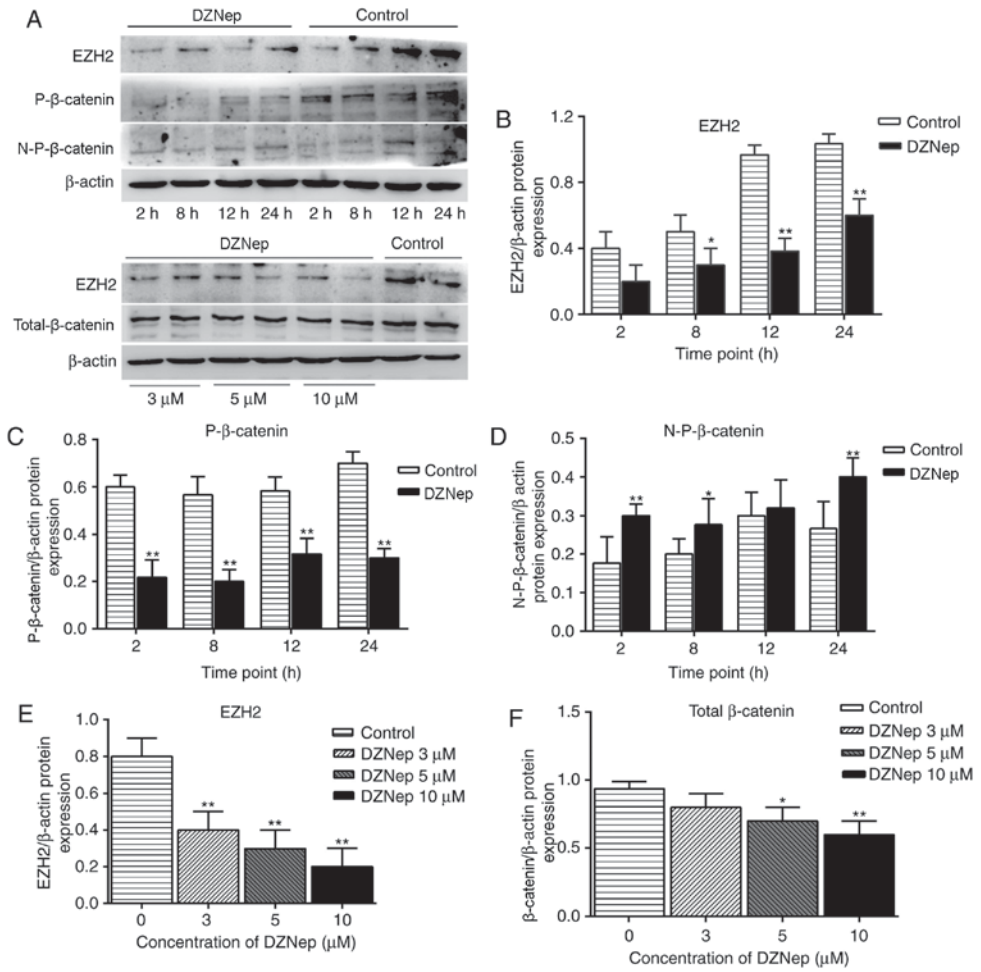

Figure 6. DZNep treatment reduces EZH2 protein expression, decreases P-β-catenin protein expression and increases N-P-β-catenin protein expression. (A) Protein expression levels of EZH2, P-β-catenin and N-P-β-catenin following 5 μM DZNep treatment for 2, 8, 12 and 24 h, and the protein expression levels of EZH2 and total-β-catenin following 3, 5 and 10 μM DZNep treatment for 24 h were detected using western blot analysis. The internal control was β-actin. (B) EZH2 expression significantly increased after 8, 12 and 24 h DZNep treatment, and the differences were statistically significant. *P<0.05 and **P<0.01 vs. respective control. Inhibition of EZH2 protein expression by DZNep was time-dependent. (C) Following 5 μM DZNep treatment in BGC-823 cells for 2, 8, 12 and 24 h, P-β-catenin significantly decreased at all time points, and the differences were statistically significant. **P<0.01 vs. respective control. (D) N-P-β-catenin significantly increased after 2, 8 and 24 h of DZNep treatment, and the differences were statistically significant. *P<0.05 and **P<0.01 vs. control. (E) Following 3, 5 and 10 μM DZNep treatment for 24 h, the EZH2 protein expression levels decreased in a dose-dependent manner. *P<0.05 and **P<0.01 vs. control. (F) Following 3, 5 and 10 μM DZNep treatment for 24 h, the total-β-catenin protein expression levels decreased in a dose-dependent manner; following 5 and 10 μM DZNep treatment in BGC-823 cells, total-β-catenin protein expression was significantly decreased. *P<0.05 and **P<0.01 vs. control. DZNep, 3-deazaneplanocin A; EZH2, enhancer of zeste homolog 2; N-P-β-catenin, non-phosphorylated β-catenin; P-β-catenin, phosphorylated β-catenin.

translocator) (32). When activated, HIF-1 mediates differential expression of genes (32). The present study is the first, to the best of our knowledge, to detect the alterations in the mRNA and protein expression levels of Hif-1α following DZNep-treatment. The results demonstrated that the relative mRNA expression level of Hif-1α significantly decreased following 1 and 5 μM DZNep-treatment for 4 h, and 5 μM DZNep-treatment for 24 h. The protein expression level of Hif-1α significantly decreased following 3, 5 and 10 μM DZNep-treatment for 2, 12 and 24 h. These results suggest that DZNep inhibited the Hif-1α protein expression level in a dose- and time-dependent manner.

Hif-1α in the microenvironment of solid tumors may induce high expression of EZH2. Chang *et al* (33) reported that in breast tumor initiating cells (BTICs), the transactivation function mediated by Hif-1α significantly upregulates EZH2 expression, whereas high EZH2 expression causes BTIC proliferation and promotes their progression. The conserved HRE sequence that interacts with Hif-1α was identified in the promoter region of EZH2, which confirmed that hypoxia induces Hif-1α to bind to this HRE region to activate EZH2 transcription, and to promote breast cancer growth (34). DZNep was the first discovered inhibitor of the enzyme activity of EZH2. Additionally, DZNep reduced the protein expression levels of EZH2 (35). The present study demonstrated that treatment with 3, 5 and 10 μM DZNep significantly reduced the protein expression level of EZH2. In addition, 5 μM DZNep significantly inhibited EZH2 expression after 8, 12 and 24 h. These results suggest that DZNep inhibited the protein expression of EZH2 in a dose- and time-dependent manner.

It has been demonstrated that EZH2 may silence a number of differentiation-associated factors, including the Gate, Sox and Pax transcription factor families, in addition to the components of the Wnt/β-catenin and transforming growth factor β signalling pathways, to cause tumor development (20,21,36). Zhang *et al* (37) revealed that β-catenin signalling and EZH2

have interactive regulation in glioblastoma. The growth inhibitory effect of EZH2 small interference RNA was reversed by dominant active β-catenin, indicating that EZH2 activates Wnt signalling to promote gastric carcinogenesis. EZH2-promoted cell growth and activation of Wnt signalling were attenuated by ectopic CXXC finger protein 4 (CXXC4) expression. EZH2 promotes the activation of Wnt signalling in gastric carcinogenesis via the downregulation of CXXC4 expression. CXXC4 is a novel potential tumor suppressor directly regulated by EZH2. Additionally, CXXC4 is a negative regulator of Wnt/β-catenin signalling (38). Inhibition of the EZH2 activity using RNA interference or small molecule inhibitors downregulates β-catenin expression. An *in vivo* study has confirmed that EZH2-knockout downregulates β-catenin expression to inhibit tumor growth (37). The mechanism is as follows: When the canonical Wnt signalling pathway is activated, secreted extracellular Wnt interacts with the transmembrane receptors LDL receptor related protein (LRP)5/6 and Frizzled to form a complex to cause the phosphorylation of the intracellular fragment of LRP5/6 and formation of the Wnt-Axin-adenomatosis polyposis coli-β-catenin complex to block β-catenin phosphorylation/degradation; free β-catenin enters into the cell nucleus and interacts with TCF/LEF to initiate the transcription of downstream genes, achieve sustained cell proliferation and induce tumors (39). Therefore, the present study used western blot analysis to detect β-catenin, P-β-catenin and N-P-β-catenin in BGC-823 cells following 3, 5 and 10 μM DZNep-treatment for 24 h. The results demonstrated that when EZH2 was inhibited, β-catenin expression also decreased. Additionally, cells were treated with DZNep for 2, 8, 12 and 24 h and expression levels of P-β-catenin and N-P-β-catenin were detected. The results demonstrated that P-β-catenin expression levels significantly decreased and NP-β-catenin expression levels significantly increased following DZNep treatment. It was speculated that DZNep may inhibit the Wnt signalling pathway to some extent to cause the degradation of accumulated P-β-catenin and an increase in N-P-β-catenin. Therefore, through the reduction of Hif-1α levels, DZNep may inhibit BGC-823 cell proliferation, promote apoptosis, reduce colony formation, and attenuate the invasion and metastasis behaviours of BGC-823 cells. The underlying action mechanism is likely to involve the inhibition of EZH2 to further block β-catenin phosphorylation.

In conclusion, the data presented in the current study indicated a positive relationship between EZH2 and Hif-1α and between EZH2 and Wnt/β-catenin signalling molecules. DZNep may inhibit the proliferation and invasion of gastric cancer cells by inhibiting EZH2 and Hif-1α expression and Wnt/β-catenin signalling. These results provide a theoretical basis for the application of DZNep in clinical trials.

Acknowledgements

Not applicable.

Funding

This work was supported by grants from the National Natural Science Foundation of China (grant no. 81460433) and the Natural Science Foundation of Ningxia Province in China (grant nos. NZ14282 and NZ14080).

Availability of data and materials

All data generated or analysed during this study are included in this published article.

Authors' contributions

RH performed the experiments and data analysis, and contributed to the writing of the manuscript. XJ performed the RT-qPCR experiments and revised the manuscript. HY performed the RT-qPCR experiments. FW performed the western blotting experiments and prepared manuscript content. YG and XC performed the data analysis and were involved in the technical aspects of the experiments. All authors read and approved the final manuscript.

Ethics approval and consent to participate

Not applicable.

Patient consent for publication

Not applicable.

Competing interests

The authors declare that they have no competing interests.

References

1. Jemal A, Bray F, Center MM, Ferlay J, Ward E and Forman D: Global cancer statistics. CA Cancer J Clin 61: 69-90, 2011.
2. Wanebo HJ, Kennedy BJ, Chmiel J, Steele G Jr, Winchester D and Osteen R: Cancer of the stomach. A patient care study by the American College of Surgeons. Ann Surg 218: 583-592, 1993.
3. Koeda K, Nishizuka S and Wakabayashi G: Minimally invasive surgery for gastric cancer: The future standard of care. World J Surg 35: 1469-1477, 2011.
4. Piunti A and Pasini D: Epigenetic factors in cancer development: Polycomb group proteins. Future Oncol 7: 57-75, 2011.
5. Gergely JE, Dorsey AE, Dimri GP and Dimri M: Timosaponin A-III inhibits oncogenic phenotype via regulation of PcG protein BMI1 in breast cancer cells. Mol Carcinog 57: 831-841, 2018.
6. Margueron R and Reinberg D: The polycomb complex PRC2 and its mark in life. Nature 469: 343-349, 2011.
7. Suvà ML, Riggi N, Janiszewska M, Radovanovic I, Provero P, Stehle JC, Baumer K, Le Bitoux MA, Marino D, Cironi L, *et al*: EZH2 is essential for glioblastoma cancer stem cell maintenance. Cancer Res 69: 9211-9218, 2009.
8. Riquelme E, Behrens C, Lin HY, Simon G, Papadimitrakopoulou V, Izzo J, Moran C, Kalhor N, Lee JJ, Minna JD and Wistuba II: Modulation of EZH2 expression by MEK-ERK or PI3K-AKT signaling in lung cancer is dictated by different KRAS oncogene mutations. Cancer Res 76: 675-685, 2016.
9. Jung HY, Jun S, Lee M, Kim HC, Wang X, Ji H, McCrea PD and Park JI: PAF and EZH2 induce Wnt/β-catenin signaling hyperactivation. Mol Cell 52: 193-205, 2013.
10. Miranda TB, Cortez CC, Yoo CB, Liang G, Abe M, Kelly TK, Marquez VE and Jones PA: DZNep is a global histone methylation inhibitor that reactivates developmental genes not silenced by DNA methylation. Mol Cancer Ther 8: 1579-1588, 2009.
11. Mochizuki D, Misawa Y, Kawasaki H, Imai A, Endo S, Mima M, Yamada S, Nakagawa T, Kanazawa T and Misawa K: Aberrant epigenetic regulation in head and neck cancer due to distinct EZH2 overexpression and dna hypermethylation. Int J Mol Sci 19: pii: E3707, 2018.

12. Yao Y, Hu H, Yang Y, Zhou G, Shang Z, Yang X, Sun K, Zhan S, Yu Z, Li P, *et al*: Downregulation of enhancer of zeste homolog 2 (EZH2) is essential for the induction of autophagy and apoptosis in colorectal cancer cells. Genes (Basel) 7: 83, 2016.
13. Wei FZ, Cao Z, Wang X, Wang H, Cai MY, Li T, Hattori N, Wang D, Du Y, Song B, *et al*: Epigenetic regulation of autophagy by the methyltransferase EZH2 through an MTOR-dependent pathway. Autophagy 11: 2309-2322, 2015.
14. Hebert M, Potin S, Sebbagh M, Bertoglio J, Bréard J and Hamelin J: Rho-ROCK-dependent ezrin-radixin-moesin phosphorylation regulates Fas-mediated apoptosis in Jurkat cells. J Immunol 181: 5963-5973, 2008.
15. Manalo DJ, Rowan A, Lavoie T, Natarajan L, Kelly BD, Ye SQ, Garcia JG and Semenza GL: Transcriptional regulation of vascular endothelial cell responses to hypoxia by HIF-1. Blood 105: 659-669, 2005.
16. Qi C, Zhang J, Chen X, Wan J, Wang J, Zhang P and Liu Y: Hypoxia stimulates neural stem cell proliferation by increasing HIF-1α expression and activating Wnt/β-catenin signaling. Cell Mol Biol (Noisy-le-grand) 63: 12-19, 2017.
17. Pang B, Zheng XR, Tian JX, Gao TH, Gu GY, Zhang R, Fu YB, Pang Q, Li XG and Liu Q: EZH2 promotes metabolic reprogramming in glioblastomas through epigenetic repression of EAF2-HIF1α signaling. Oncotarget 7: 45134-45143, 2016.
18. Chen Q, Cai J, Wang Q, Wang Y, Liu M, Yang J, Zhou J, Kang C, Li M and Jiang C: Long noncoding RNA NEAT1, regulated by the EGFR pathway, contributes to glioblastoma progression through the WNT/β-catenin pathway by scaffolding EZH2. Clin Cancer Res 24: 684-695, 2018.
19. Livak KJ and Schmittgen TD: Analysis of relative gene expression data using real-time quantitative PCR and the 2(-Delta Delta C(T)) method. Methods 25: 402-408, 2001.
20. Panousis D, Patsouris E, Lagoudianakis E, Pappas A, Kyriakidou V, Voulgaris Z, Xepapadakis G, Manouras A, Athanassiadou AM and Athanassiadou P: The value of TOP2A, EZH2 and paxillin expression as markers of aggressive breast cancer: Relationship with other prognostic factors. Eur J Gynaecol Oncol 32: 156-159, 2011.
21. Choi JH, Song YS, Yoon JS, Song KW and Lee YY: Enhancer of zeste homolog 2 expression is associated with tumor cell proliferation and metastasis in gastric cancer. Apmis 118: 196-202, 2010.
22. Cheng LL, Itahana Y, Lei ZD, Chia NY, Wu Y, Yu Y, Zhang SL, Thike AA, Pandey A, Rozen S, *et al*: TP53 genomic status regulates sensitivity of gastric cancer cells to the histone methylation inhibitor 3-deazaneplanocin A (DZNep). Clin Cancer Res 18: 4201-4212, 2012.
23. Chang CJ, Yang JY, Xia W, Chen CT, Xie X, Chao CH, Woodward WA, Hsu JM, Hortobagyi GN and Hung MC: EZH2 promotes expansion of breast tumor initiating cells through activation of RAF1-catenin signaling. Cancer Cell 19: 86-100, 2011.
24. Glazer RI, Hartman KD, Knode MC, Richard MM, Chiang PK, Tseng CK and Marquez VE: 3-Deazaneplanocin: A new and potent inhibitor of S-adenosylhomocysteine hydrolase and its effects on human promyelocytic leukemia cell line HL-60. Biochem Biophys Res Commun 135: 688-694, 1986.
25. Liu S, Liu F, Huang W, Gu L, Meng L, Ju Y, Wu Y, Li J, Liu L and Sang M: MAGE-A11 is activated through TFCP2/ZEB1 binding sites de-methylation as well as histone modification and facilitates ESCC tumor growth. Oncotarget 9: 3365-3378, 2017.
26. Sha M, Mao G, Wang G, Chen Y, Wu X and Wang Z: DZNep inhibits the proliferation of colon cancer HCT116 cells by inducing senescence and apoptosis. Acta Pharm Sin B 5: 188-193, 2015
27. Huang Y, Lin D and Taniguchi CM: Hypoxia inducible factor (HIF) in the tumor microenvironment: Friend or foe? Sci China Life Sci 60: 1114-1124, 2017.
28. Martin JD, Fukumura D, Duda DG, Boucher Y and Jain RK: Reengineering the tumor microenvironment to alleviate hypoxia and overcome cancer heterogeneity. Cold Spring Harb Perspect Med 6: pii: a027094, 2016.
29. Li DW, Dong P, Wang F, Chen XW, Xu CZ and Zhou L: Hypoxia induced multidrug resistance of laryngeal cancer cells via hypoxia-inducible factor-1α. Asian Pac J Cancer Prev 14: 4853-4858, 2013.
30. Borsi E, Terragna C, Brioli A, Tacchetti P, Martello M and Cavo M: Therapeutic targeting of hypoxia and hypoxia-inducible factor 1 alpha in multiple myeloma. Transl Res 165: 641-650, 2015.
31. Lou JJ, Chua YL, Chew EH, Gao J, Bushell M and Hagen T: Inhibition of hypoxia-inducible factor-1alpha protein synthesis by DNA damage inducing agents. PLoS One 5: e10522, 2010.
32. Michel G, Minet E, Ernest I, Durant F, Remacle J and Michiels C: Molecular modeling of the hypoxia-inducible factor-1 (HIF-1). Theor Chem Acc 101: 51-56, 1999.
33. Chang CJ, Yang JY, Xia W, Chen CT, Xie X, Chao CH, Woodward WA, Hsu JM, Hortobagyi GN and Hung MC: EZH2 promotes expansion of breast tumor initiating cells through activation of RAF1-β-catenin signaling. Cancer Cell 19: 86-100, 2011.
34. Mahara S, Lee PL, Feng M, Tergaonkar V, Chng WJ and Yu Q: HIFI-α activation underlies a functional switch in the paradoxical role of Ezh2/PRC2 in breast cancer. Proc Natl Acad Sci USA 113: E3735-E3744, 2016.
35. Tan J, Yang X, Zhuang L, Jiang X, Chen W, Lee PL, Karuturi RK, Tan PB, Liu ET and Yu Q: Pharmacologic disruption of Polycomb-repressive complex 2-mediated gene repression selectively induces apoptosis in cancer cells. Genes Dev 21: 1050-1063, 2007.
36. Tsang DP and Cheng AS: Epigenetic regulation of signaling pathways in cancer: Role of the histone methyltransferase EZH2. J Gastroenterol Hepatol 26: 19-27, 2011.
37. Zhang J, Chen L, Han L, Shi Z, Zhang J, Pu P and Kang C: EZH2 is a negative prognostic factor and exhibits pro-oncogenic activity in glioblastoma. Cancer Lett 356: 929-936, 2015.
38. Lu H, Sun J, Wang F, Feng L, Ma Y, Shen Q, Jiang Z, Sun X, Wang X and Jin H: Enhancer of zeste homolog 2 activates Wnt signaling through downregulating CXXC finger protein 4. Cell Death Dis 4: e776, 2013.
39. Minde DP, Radli M, Forneris F, Maurice MM and Rüdiger SG: Large extent of disorder in Adenomatous Polyposis Coli offers a strategy to guard Wnt signalling against point mutations. PLoS One 8: e77257, 2013.